ADVANCED OPTICAL MATERIALS

PHOTOLUMINESCENCE

Leveraging on plasmonic hot electrons is an emerging strategy for electron–hole separation towards efficient photovoltaics and photocatalysis. On page 960, X. Huang, S. J. Wang, S. J. Chua, and co-workers extend this concept to electron–hole recombination for illumination, which is rarely reported. By taking advantage of the good energy match between the dopant-correlated green luminescence in Cu-doped ZnO nanowires and the localized surface plasmon resonance of Au nanoparticles, an intense, ultrafast, and temperature-robust UV luminescence is achieved in the nanowires after coating with Au nanoparticles.

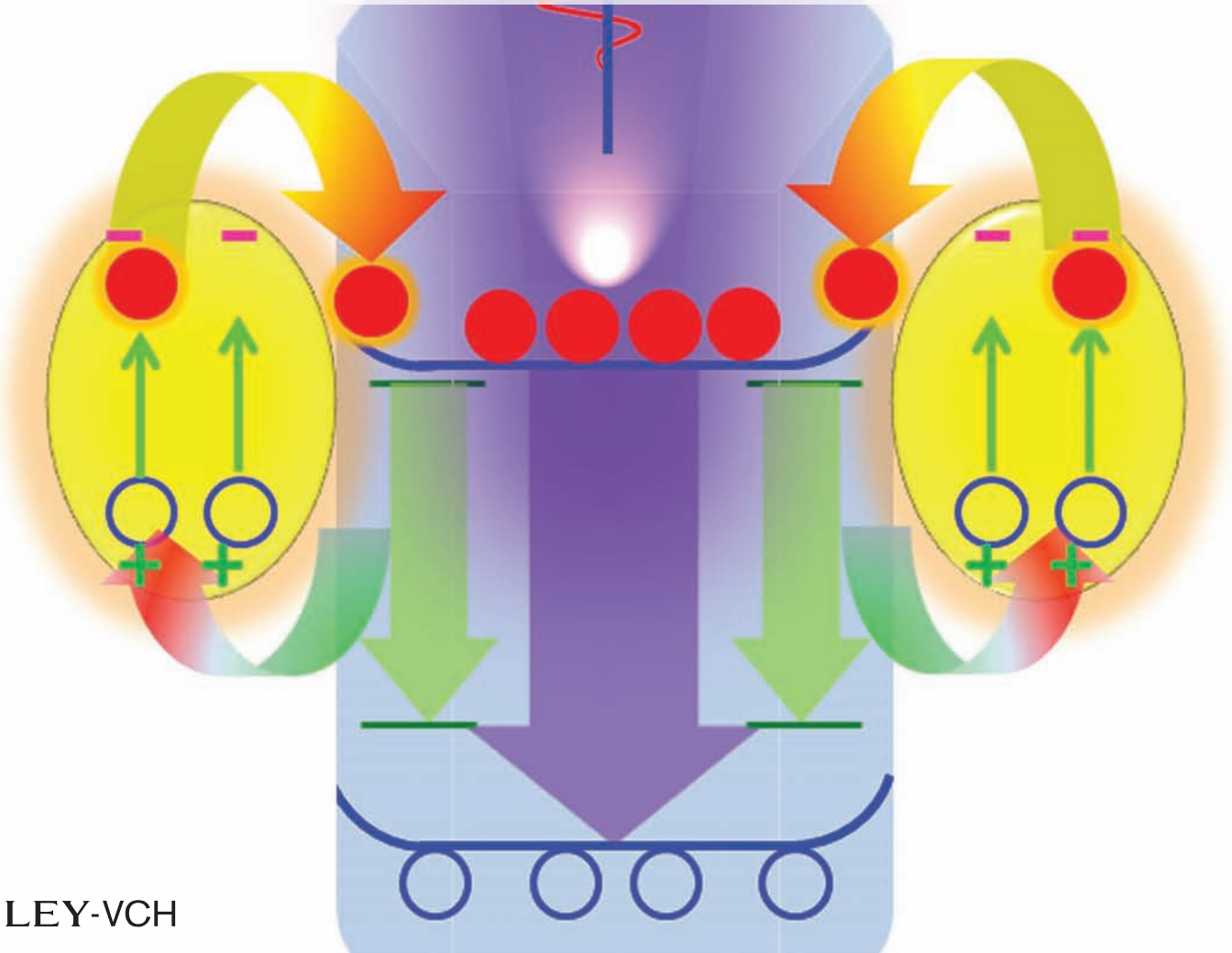

WILEY-VCH

ADVANCED OPTICAL MATERIALS
www.advopticalmat.de

Materials Views
www.MaterialsViews.com

Ultrafast and Robust UV Luminescence from Cu-Doped ZnO Nanowires Mediated by Plasmonic Hot Electrons

Xiaohu Huang, Rui Chen, Chen Zhang, Jianwei Chai, Shijie Wang,* Dongzhi Chi, and Soo Jin Chua**

Leveraging on plasmonic hot electrons is regarded as an emerging strategy for electron–hole separation toward efficient photovoltaics and photocatalysis, but its application in electron–hole recombination for illumination is rarely explored. Herein, a significantly improved ultraviolet luminescence is reported from Cu-doped ZnO nanowires (NWs) through dopant mediated generation and transfer of plasmonic hot electrons. Through coupling the Cu dopants-correlated green luminescence in Cu-doped ZnO NWs with the localized surface plasmon resonance of Au nanoparticles (NPs), UV emission from the NWs is enhanced by a factor of ≈280 and its lifetime drops from 2.45 ns to about 18 ps after covering the NWs with Au NPs. Moreover, robust UV emission sustains from room temperature to low temperature. This work extends the applications of plasmonic hot electrons and provides an appealing route toward achieving intense, ultrafast, and temperature-robust luminescence, which holds great potential in light-emitting diode and laser diodes for illumination, optical communication, and biomedical applications.

1. Introduction

Coupling the exciton of semiconductor nanowires (NWs) with surface plasmon (SP) of metal films or nanoparticles (NPs) accelerates the light–matter interaction, thus creates an unprecedented opportunity toward achieving intense and ultrafast photonic emission.[1–3] In addition, the conducting nature of the metal coating facilitates seamless electrical contacts,[4] which is particularly important for the applications of the semiconductor NWs in light-emitting diodes (LEDs)[1] and laser diodes.[5] Therefore, toward high performance NWs solid state lighting, SP-enhanced route[6] stands out among the other strategies, namely, surface passivation,[7] hydrogen doping,[8] and exciton localization.[9]

ZnO semiconductor with a bandgap of 3.37 eV and a large exciton binding energy of 60 meV is regarded as a promising ultraviolet (UV) luminescent material.[10,11] However, the UV emission from ZnO nanostructures is found to be weaker than expected because of various defects incorporated during growth, which results in a broad defect emission band in the visible region,[12] and this is especially true for solution-grown ZnO nanomaterials.[11–15] Metal NPs coating has been extensively explored as an effective way to enhance the UV photoluminescence (PL) of ZnO nanomaterials.[6,16–18] However, inevitable oxidation of many of the metal NPs (e.g., Ag and Al) deteriorates their practical performance far below their theoretical predictions.[19] Thus Au NPs are widely used in plasmonics because of their resistance to oxidation, although their localized surface plasmon resonance (LSPR) absorption spectra fall mainly in the visible light range in most cases,[20] which does not match the UV PL of ZnO very well. Recently, the reported similar enhancement of UV PL from ZnO by coating with different metal NPs (including Au, Ag, Pt, and Al) with varied LSPR characteristics casts doubt on the underlying mechanism of luminescence enhancement.[17] So far, the reports on SP-enhanced luminescence are mainly based on direct coupling between the LSPR of metal NPs and luminescence-of-interest from semiconductors. However, this route leads to substantial self-absorption of the emitted light by the metal NPs,[21] thus compromising the initial objective of enhancing the luminescence. Moreover, contrary to the luminescence enhancement at room temperature, it was shown that the UV luminescence from metal-NPs-coated ZnO is suppressed at low temperature.[18,22] Thus, overcoming the limitations of luminescence self-absorption and low temperature suppression has far-reaching impact not only on fundamental science but also on practical applications.

Although plasmonic hot electrons have been documented in photovoltaics, photocatalysis, and photodetectors,[23–25] their potential in luminescence enhancement has yet to be explored.

Dr. X. H. Huang, Dr. J. W. Chai, Dr. S. J. Wang, Dr. D. Z. Chi, Prof. S. J. Chua
Institute of Materials Research and Engineering
Agency for Science, Technology and Research (A*STAR)
Singapore 138634, Singapore
E-mail: huangxh@imre.a-star.edu.sg; sj-wang@imre.a-star.edu.sg
Prof. R. Chen
Department of Electrical and Electronic Engineering
South University of Science and Technology of China
Shenzhen 518055, China
Dr. C. Zhang
Department of Materials Science and Engineering
Massachusetts Institute of Technology
Cambridge, MA 02139, USA
Prof. S. J. Chua
Department of Electrical and Computer Engineering
National University of Singapore
Singapore 117576, Singapore
E-mail: elecsj@nus.edu.sg

DOI: 10.1002/adom.201600026

Herein, we propose to address the above mentioned challenges in SP-enhanced luminescence via dopants-mediated generation and transfer of plasmonic hot electrons. Taking ZnO NWs as an example, the strong green luminescence (GL) from Cu dopants[26] lies exactly in the LSPR absorption spectrum of Au NPs.[20] Through resonant coupling between the GL and LSPR, plasmonic hot electrons are generated and transferred from Au NPs to the conduction band of Cu-doped ZnO NWs,[27] resulting in a significantly enhanced UV emission with an extremely shortened radiation lifetime from the NWs. To the best of our knowledge, this is the first report on doping mediated plasmonic enhancement of the UV luminescence from ZnO. Moreover, our strategy allows for UV enhancement over a wide temperature range. The results show that leveraging on the plasmonic hot electrons is a promising approach toward fabricating high performance LED and laser diodes.

2. Result and Discussion

2.1. Characterizations of the Cu-Doped ZnO NWs Coated with Au NPs

Morphology of the Cu-doped ZnO NWs is shown in the scanning electron microscopy (SEM) image in **Figure 1**a. The diameter of the NWs ranges from 50 to 100 nm, and the length of the NWs is about 1 μm. A typical transmission electron microscopy (TEM) image of the NW is shown in Figure 1b. Selective area electron diffraction (SAED) pattern in the inset of Figure 1b indicates that the NW is single crystalline ZnO with wurtzite structure, grown along (002) *c*-axis. Metal NPs were sputtered onto the NWs, which can be seen from the SEM image in Figure 1c. The lattice distance of the NPs is measured to be 0.235 nm from the high-resolution transmission electron microscope (HRTEM) image in Figure 1d, corresponding to the (111) plane of Au with face-centered-cubic structure. The shape of the NPs is close to an ellipsoid. The size of the NPs is defined by the length across the longer side of the NPs, which corresponds to the plasmonic length of the NPs.[28] As seen from Figure 1d, the size of the NPs varies from 3 to 15 nm, thus the size mentioned in the following text is an estimated average value. X-ray diffraction (XRD) pattern (Figure 1e) of the NWs can be well indexed to hexagonal wurtzite ZnO (JCPDF No. 89-1397), and is consistent with the SAED result. Secondary ion mass spectrometry (SIMS) results clearly indicate the presence of Cu in the doped NWs (Figure 1f), although Cu-related precipitates were not detected by XRD and TEM.

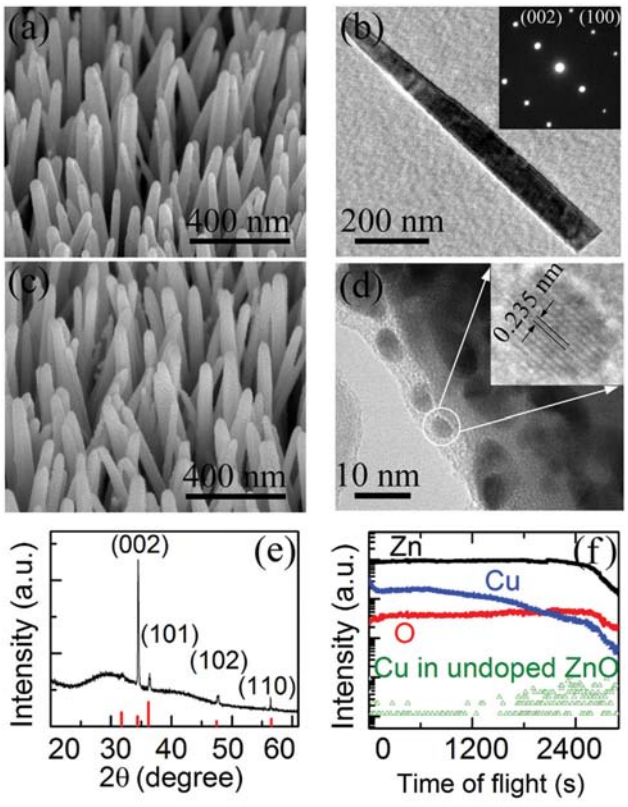

Figure 1. a) SEM image and b) TEM image with an inset of SAED pattern of Cu-doped ZnO NWs without Au NPs, c) SEM image and d) TEM image with an inset of the HRTEM image showing the Au NP of Cu-doped ZnO NWs covered with Au NPs, e) XRD and f) SIMS spectra of Cu-doped ZnO NWs without Au NPs.

2.2. Giant UV Luminescence Enhancement

Figure 2 compares the effect of Au NPs on the PL spectra of undoped and Cu-doped ZnO NWs at room temperature. Similar to previous reports,[12,14,15] the PL spectrum of undoped ZnO exhibits a UV emission around 377 nm from near-band-edge

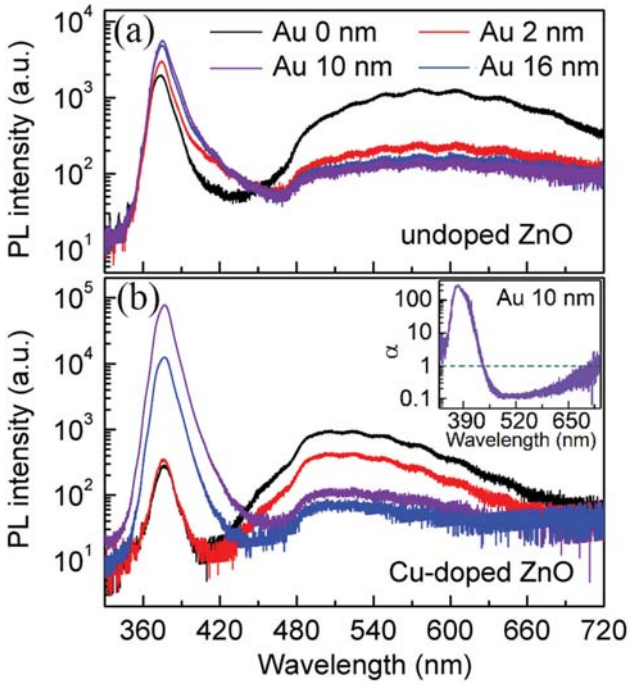

Figure 2. PL spectra of a) undoped ZnO NWs and b) Cu-doped ZnO NWs measured under identical condition, Au NPs with different size were coated onto the NWs. The inset in (b) is the enhancement factor versus wavelength for Cu-doped ZnO NWs coated with 10 nm Au NPs.

emission and a broad defects emission around 580 nm. The defects emission normally originates from intrinsic defects such as oxygen vacancies and oxygen interstitials.[13,14] After coating with Au NPs, the defects emission weakens and the UV emission strengthens as shown in Figure 2a. The intensity of the UV emission is enhanced by only a few times even with an optimized size (≈10 nm) of Au NPs, similar to many of the previous reports.[6,18,22,29] After doping with Cu, the PL spectra of the NWs show a relatively weak UV emission and a strong GL centered at ≈502 nm,[26] which is consistent with previous findings.[30] As shown in Figure 2b, upon coating with Au NPs onto the Cu-doped ZnO NWs, the GL weakens substantially, while the UV emission strengthens dramatically. In contrast to the undoped ZnO, the enhancement factor (α)[8] of the UV emission in Cu-doped ZnO can be as high as 280 with an optimized size of Au NPs around 10 nm (the inset of Figure 2b), which is two orders of magnitude larger than the fluctuation caused by nonuniformity of the samples (Figure S1, Supporting Information).

2.3. Shortened UV Luminescence Lifetime

In order to shed light on the mechanism of the UV enhancement, time-resolved photoluminescence (TRPL) spectra of the Cu-doped ZnO NWs are shown in **Figure 3**. The decay curve of the UV emission from Cu-doped ZnO NWs without Au NPs can be well fitted with a bi-exponential function with time constants $\tau_1 = 0.52 \pm 0.03$ ns and $\tau_2 = 2.45 \pm 0.09$ ns. The amplitude of the fast decay is typically ≈23% of the total decay. The fast decay component exhibits a time constant comparable to that of ZnO NWs in the literatures (≈0.45 ns),[18] and is commonly attributed to the excitons on the surface of ZnO, where nonradiative recombination via surface states leads to a fast decay.[18,31,32] The slow decay component has a time constant close to that of bulk ZnO (≈3 ns), and is ascribed to the intrinsic radiation of free excitons (FX).[32] In sharp contrast, after covering Au NPs on the Cu-doped ZnO NWs, the decay curve exhibits a single exponential decay behavior. Subtracting the instrument response function from the decay curve yields an estimation of the lifetime of the UV emission to be about 18 ps, which is among the shortest for spontaneous emission ever reported in ZnO.[6,18,33] The dramatic reduction in the lifetime of the UV emission translates to a Purcell factor as high as ≈136. This comparison suggests unambiguously that the enhancement of UV emission from Cu-doped ZnO NWs after coating with Au NP is not due to surface passivation, as suppression of surface nonradiative recombination leads to longer decay time of the UV emission,[29] which is contrary to what we have observed here. The shortened radiative lifetime is in good agreement with the scenario of LSPR enhanced UV emission,[34] which may be originated from an additional decay channel through electron–hole–SP coupling.[29]

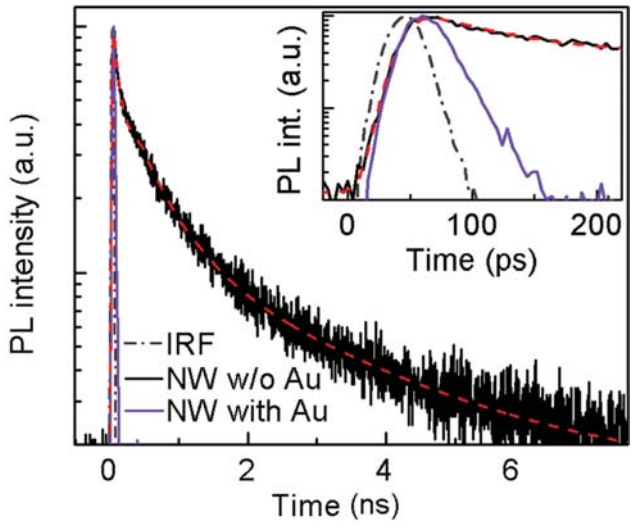

Figure 3. TRPL spectra of Cu-doped ZnO NWs with and without Au NPs, and the inset is the enlarged part in the short time region. The IRF is the instrument response function, which restricts the detection limit of the system.

2.4. Temperature-Robust UV Luminescence Enhancement

The UV enhancement is further studied by low temperature PL measurements. For comparison, the variable temperature PL spectra of Cu-doped ZnO NWs before and after coating Au NPs are depicted in **Figure 4**. The UV emission from bare Cu-doped ZnO NWs at 18 K is dominated by radiative recombination from donor-bound excitons (DX) located at 3.359 eV, and the feature of FX emission can be well observed. Moreover, a clear peak at 3.31 eV as well as its longitudinal optical phonon replicas can be distinguished. Different from the FX and DX, the position of this set of peaks seems to be weakly temperature dependent on the measurement temperature (Figure 4a), being coincidently similar to the behavior of GL (Figure 4a).[26] The 3.31 eV peak was also observed to be weakly temperature dependent in ZnO quantum dots,[35] and it was normally ascribed to acceptor-related excitons,[36] thus here we tentatively ascribe it to radiative recombination from acceptor-bound excitons (AX) related to zinc vacancies or Cu dopants. In contrast, the Cu-doped ZnO NWs coated with Au NPs only exhibit an emission at 3.361 eV without clear fine structures in the UV range (Figure 4b). Figure 4c shows the PL spectra of Cu-doped ZnO NWs with and without Au NPs measured at 18 K. The Arrhenius plots of the integrated PL intensity of Cu-doped ZnO NWs as a function of measurement temperature are shown in Figure 4d. Clearly, the UV enhancement in Cu-doped ZnO NWs coated with Au NPs persists from room temperature to low temperature. This finding is in sharp contrast to the disappearance of UV enhancement at low temperature in undoped ZnO NWs coated with either Ni NPs or Au NPs in the previous reports.[18,22]

2.5. Excitation-Power-Dependence of the Improved UV Luminescence

To have a better understanding on the improved UV luminescence, **Figure 5**a shows the PL spectra of Cu-doped ZnO NWs coated with 10 nm Au NPs under different excitation power of the laser source. With the laser power increases from 0.074 to 100 mW, the UV luminescence strengthens without clear peak

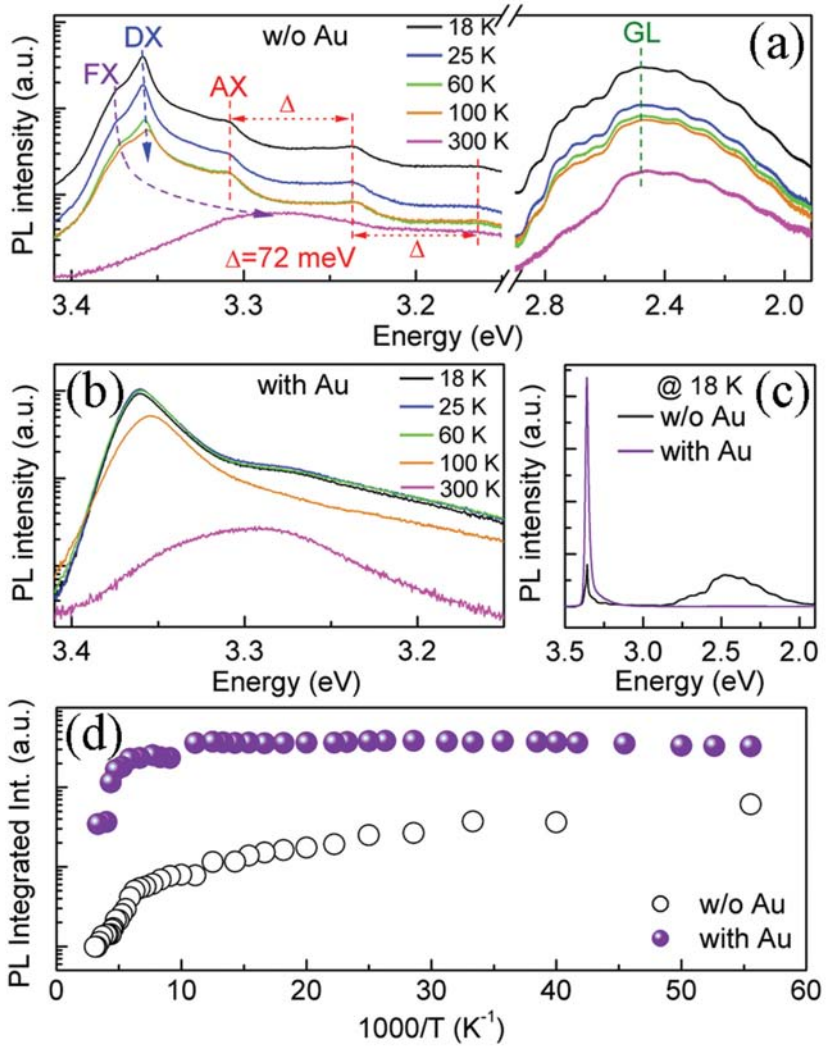

Figure 4. Variable temperature PL spectra of a) bare Cu-doped ZnO NWs and b) Cu-doped ZnO NWs with Au NPs. c) Comparison of low temperature (at 18 K) PL spectra of Cu-doped ZnO NWs with and without Au NPs, respectively. d) Arrhenius plot of the UV emission of Cu-doped ZnO NWs with and without Au NPs, respectively.

shift. As shown in Figure 5b, the integrated intensity of the UV luminescence follows a linear power-dependence behavior with the excitation power, which is in line with that of spontaneous emission.[37] Consistent with previous results on ZnO,[35] the power factor k is 1.15 ± 0.02, which falls into the range of 1–2 and is quite close to 1, most likely corresponding to FX emission.[37] For comparison, the integrated intensity of UV luminescence and GL from bare Cu-doped ZnO NWs are also plotted in Figure 5b, which also follow a similar linear power-dependence behavior. The power factor for the UV emission from bare Cu-doped ZnO NWs is 1.39 ± 0.12, which is quite close to 1.5, indicating besides FX, bound excitons may also make a significant contribution to the UV luminescence of the bare NWs.[37] The power factor for the GL from bare Cu-doped ZnO NWs is 0.94 ± 0.02, which is below 1. Such a power factor suggests the nature of the GL in bare Cu-doped ZnO is free-to-bound radiative recombination,[37] which is in agreement with the previous ascription of the GL.[30,38]

2.6. Mechanism of UV Luminescence Enhancement

A possible mechanism of the UV luminescence enhancement from Cu-doped ZnO NWs is proposed, which involves the following steps: First, upon excitation by a 325 nm laser, an ultrafast charge transfer from the ZnO host to the Cu dopants happens followed by carriers recombination at the Cu dopants, which will generate GL if there is no Au NPs.[38] Second, the energy of the LSPR absorption of Au NPs overlaps with the energy of the GL so well (**Figure 6**a) that the energy from the GL of Cu-doped ZnO can transfer to the LSPR of Au NPs, probably through Förster resonance energy transfer,[39] in which the energy transfer may happen instantaneously with the carrier recombination without physically generating the GL photon. This energy transfer process is manifested by the disappearance of GL in Cu-doped ZnO after covering Au NPs. Third, nonradiative decay of the LSPR of Au NPs generates excited electrons, typically referred to as plasmonic hot electrons.[24,27] Fourth, calculation results show long lifetime of the hot electrons corresponding to a high efficiency of plasmon-induced energetic hot electrons,[40] considering the lifetime of the hot electrons at the surface of Au NPs is as long as 1–3 ps,[41] it is reasonable to deduce that many of the plasmonic hot electrons have enough energy to overcome the Schottky barrier between Cu-doped ZnO NWs and Au NPs (≈0.66 eV) (Supporting Information).[40,42] Therefore, it is thermodynamically favored for many of the hot electrons to inject from the Au NPs to the conduction band of Cu-doped ZnO, as demonstrated in photovoltaic and photocatalytic systems.[24,43] Especially the lifetime of the hot electrons at the surface of Au NPs is 1–3 ps,[41] which is one order of magnitude longer than the time scale of hot electrons injection process (approximately hundreds of femtoseconds),[44,45] thus providing enough time to accommodate the electron transfer process. These processes together with the energy band alignment between Cu-doped ZnO NWs and Au NPs are schematically illustrated in Figure 6b.[24,33,46] In other words, the energy transfer process (from Cu-doped ZnO NWs to Au NPs) and the hot electron transfer process (from Au NPs to Cu-doped ZnO NWs) turn the Au NPs into "electron pumps," which generate plasmonic hot electrons and transfer them to the conduction band of Cu-doped NWs within a very short period of time. The transferred hot electrons from the Au NPs increase electron density in the conduction band of Cu-doped ZnO NWs, leading to an increase in the spontaneous emission rate of exciton,[47] as manifested by the shortened UV PL decay time shown in Figure 3. We note that besides the intensity enhancement, the UV peak of the

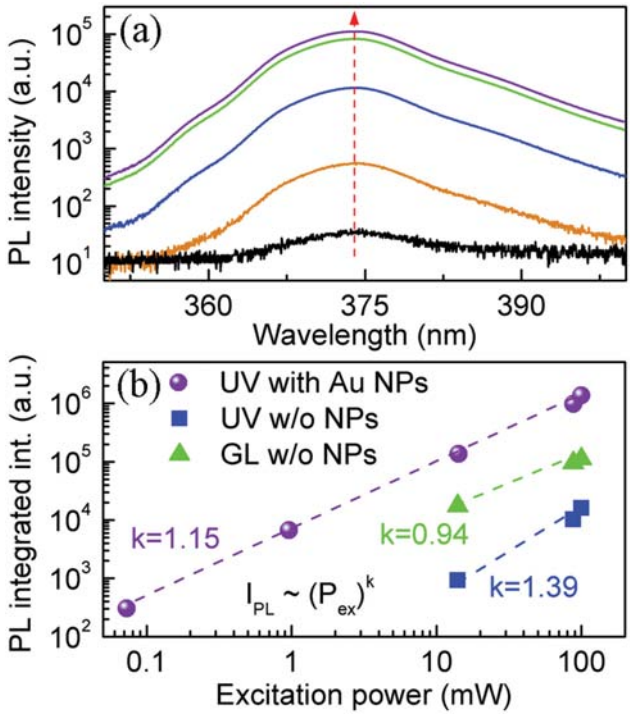

Figure 5. a) Room temperature PL spectra of Cu-doped ZnO NWs coated with 10 nm Au NPs under different excitation power ranging from 0.07 to 100 mW. b) Log–log plot of the integrated PL intensity (I_{PL}) of the UV luminescence shown in (a) as a function of the excitation power (P_{ex}). For comparison, the results of UV luminescence and GL from bare Cu-doped ZnO NWs are also included.

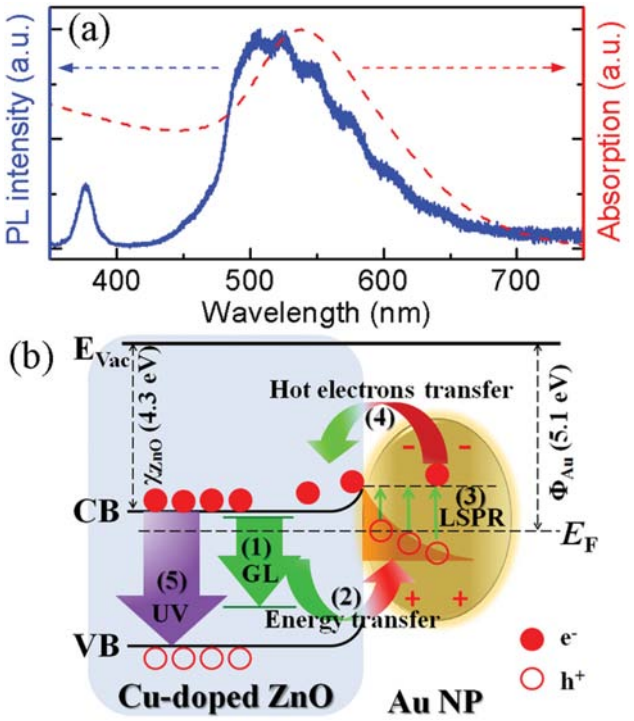

Figure 6. a) Comparison between the PL spectrum of bare Cu-doped ZnO NWs and the absorption spectrum of Au NPs with a size of 10 nm. b) Schematic illustration of the possible mechanism of the UV enhancement involving the processes of 1) virtually generating GL at Cu dopant, 2) transferring energy from the virtual GL of Cu-doped ZnO NWs to LSPR of Au NPs, 3) exciting LSPR of Au NPs upon receiving the transferred energy from the virtual GL, and generating plasmonic hot electrons as a result of nonradiative decay of the LSPR, 4) transferring hot electrons from Au NPs to the conduction band of Cu-doped ZnO NWs, and 5) excitons radiative recombination at Cu-doped ZnO into UV emission. The energy band alignment between Cu-doped ZnO NWs and Au NPs is sketched approximately according to refs.[24,33] and[46].

NWs broadens after coating with metal NPs (Figure 2b). This could be due to increased concentration of electrons on the surface of the NWs,[15] which is in line with the scenario of carriers accumulation on the surface of the NWs due to transfer of hot electrons from the metal NPs to the NWs.

2.7. Further Discussion

It is noted that the peak position of LSPR absorption maximum varies with the size of the Au NPs. With prolonging the sputtering time of Au, the size of Au NPs increases, which leads to a redshift of the LSPR peak position (Figure S2, Supporting Information).[20,28] Decreasing or increasing the Au NPs size will shift the LSPR maximum away from the GL spectrum maximum, thus deviating from a perfect energy match to fulfill the resonance condition. The optimal size of the Au NPs to achieve the strongest UV emission from Cu-doped ZnO NWs is about 10 nm, at which the corresponding LSPR absorption[20,28] matches well with that of the GL (Figure 6a). The importance of the resonant coupling is further manifested by the PL spectra of Cu-doped ZnO NWs coated with Pt NPs (Figure S3, Supporting Information). The UV enhancement factor is one order of magnitude smaller for NWs coated with Pt NPs than that for NWs coated with Au NPs, as a resonant coupling between the LSPR of 10 nm Pt NPs and the GL cannot be established due to the LSPR energy of the Pt NPs being in the UV region[48] rather than green light range.

It is worthy to note that the decay time of the enhanced UV luminescence in our work is only about 18 ps (Figure 3). To the best of our knowledge, it is among the shortest for spontaneous emission in metal-NPs-decorated ZnO nanomaterials (e.g., ≈30 ps in ZnO nanorods capped by Au NPs,[6] 50 ps in ZnO NWs coated with Ni NPs,[18] 64 ps in ZnO nanoparticles coupled with Au NPs,[33] and 261 ps in ZnO NWs coated with Au NPs[17]). The decay time of the improved UV luminescence is one order of magnitude longer than that of the stimulated emission in ZnO (≈1 ps[49,50]), which is in line with its nature of spontaneous emission as revealed by the power-dependent results in Figure 5. The short lifetime of 18 ps corresponds to a frequency of about 55 GHz, which shows great potential in high speed optical communication. Another significant feature of the enhanced UV emission achieved by Cu dopants-mediated generation and transfer of plasmonic hot electrons is its excellent temperature stability at low temperature, which is in sharp contrast to the disappearance of UV enhancement at low temperature in undoped ZnO NWs coated with either Ni NPs or Au NPs in the literature.[18,22] Prior reports on SP-enhanced luminescence are widely based on the guiding principle of direct coupling between LSPR and

luminescence-of-interest,[1,6,18] where the enhancement of UV emission from ZnO decorated with metal NPs at room temperature is ascribed to a strong coupling between LSPR and FX.[18] However at low temperature, bound excitons (DX and AX) emission dominates the PL spectra (see Figure 4a), and their coupling with the LSPR is believed to be weak probably due to their weak oscillation strength and localization nature.[18] In addition to the self-absorption by the metal NPs themselves, strong UV emission from ZnO NWs/metal NPs system at low temperature was rarely documented in the literature.[4] Herein we find that the limitation of direct coupling between the LSPR and the UV emission from ZnO can be circumvented by leveraging on the plasmonic hot electrons through coupling the LSPR with the carrier recombination at the dopants. It was suggested that the coupling mechanism between exciton and LSPR may be similar to that between exciton and phonon.[51] The structured GL with multiple phonon replica in Cu-doped ZnO[26] (Figure 4a) infers that the coupling between GL exciton and phonon is quite strong, thus it is reasonable to expect a strong coupling between GL exciton and LSPR when coating Au NPs onto Cu-doped ZnO NWs, although the GL photon may not necessarily to be generated. By assuming an internal quantum efficiency (IQE) ≈100% at 18 K,[8] the IQE of the UV emission from Cu-doped ZnO NWs at 300 K is increased from 1.6% to 11% after coating with Au NPs.

The UV enhancement of undoped ZnO NWs after coating with metal NPs (Figure 2a) is mainly caused by surface passivation, as evidenced by the prolonged exciton lifetime revealed in previous reports.[29] Enhanced light scattering/extraction may also play a part in enhancing the UV emission. These factors are believed to account for the difference between the Purcell factor (≈136) and the UV enhancement factor (≈280) in our results on Cu-doped ZnO NWs coated with Au NPs. Besides, in undoped ZnO coated with Au NPs, the photon-excited electrons in the conduction band of ZnO could tunnel through the Schottky barrier to the adjacent Au NPs, which facilitates electron–hole separation and could suppress the UV emission if the Au NPs are attached on the side walls of the ZnO NWs.[52] However, the electrons tunneling through the Schottky barrier can be prevented after doping Cu into ZnO, since Cu dopants can trap the electrons effectively through forming acceptor centers. The formation of acceptor centers in Cu-doped ZnO NWs is manifested by the formation of additional band tail states in the X-ray photoelectron spectrometry (XPS) valence band spectrum compared to that in the undoped ZnO (Figure S4, Supporting Information).[53] The electrons can transfer from the ZnO host to the Cu dopants in a timescale as short as ≈40 ps,[38] and this process is thermodynamically more favorable than tunneling through a Schottky barrier to the adjacent Au NPs. These comparisons further highlight the vital roles of Cu dopants and also differentiate our results from the previous ones based on undoped ZnO.[6,16–18,22,33,41,52,54,55]

It should be noted that the LSPR of Au NPs could be excited coincidentally through the defects-correlated visible emission in ZnO,[33,47,54,55] however the poor thermal stability of these defects[14,15] makes such an alternative not reliable in practical applications. Here we propose a new strategy to address this issue by taking advantage of the thermally stable Cu dopants in ZnO.[26] The UV luminescence from our NWs integrates the merits of high intensity, ultra-short lifetime, and temperature-robust characteristic, which are highly desirable in nanoscale LED and laser diodes.[2] It opens up opportunities to tailor the coupling between the LSPR of metal NPs and the exciton of semiconductor through chemical doping. The concept that utilizing dopants to mediate the generation and transfer of plasmonic hot electrons provides a new avenue to modify the SP–exciton coupling and charge transfer at the interface of metal NPs and semiconductors NWs, which are critical to maximize the potential of plasmonic hot electrons in photonics and beyond.[24,43,56]

3. Conclusion

In conclusion, we report an extraordinary UV luminescence from Cu-doped ZnO NWs by dopants mediated generation and transfer of plasmonic hot electrons. SP–exciton resonant coupling is achieved through matching the LSPR absorption of Au NPs with the Cu-correlated GL of Cu-doped ZnO NWs, as manifested by the suppression of GL from Cu-doped ZnO NWs after coating Au NPs. Meanwhile, UV emission from the NWs is enhanced remarkably, and the lifetime of the UV emission is shortened from about 2.4 ns to 18 ps, corresponding to a Purcell factor as large as 136. Moreover, the enhanced UV emission shows robust temperature stability down to 18 K. The NWs with intense, ultrafast, and temperature-robust UV emission hold great potential in nanoscale UV LED and laser diodes.

4. Experimental Section

Synthesis of NWs and Metal NPs Coating: A chemical bath deposition method was adopted to synthesize Cu-doped ZnO NWs on Si (100) substrates.[26] Briefly, a seed layer of ZnO NPs was spin-coated onto the substrates, followed by annealing in air at 250 °C for half an hour. The growth solution consisted of 25×10^{-3} M zinc acetate and 1×10^{-3} M copper acetate in deionized water, in which ammonia was added to adjust the pH value to about 10. The growth was conducted at 90 °C at ambient pressure for 1 h. The NWs were annealed at 800 °C in air for 30 min to promote the formation of substituted Cu dopants at Zn site, as evidenced by the Cu-related strong GL from the samples after annealing.[26] Reference samples of undoped ZnO NWs were synthesized by the same procedures except without copper acetate in the growth solution. Metal (Au or Pt) NPs were sputtered onto the NW by direct-current sputter (JEOL JFC-1600 Auto Fine Coater) at a sputtering rate of ≈0.3 nm s^{-1}, and the average size of the NPs was controlled by adjusting the sputtering time.

Characterization and Luminescence Measurements of NWs: The structure, morphology, and composition of the samples were characterized by XRD (Bruker D8 Discover), SEM (Helios Nanolab 600), TEM (JEOL JEM 2100), and SIMS (TOF-SIMS IV). UV–visible absorption spectra were scanned by UV-3600 UV–Vis–NIR Spectrophotometer (Shimadzu). PL spectra were recorded using a micro-PL system (Renishaw Ramanscope 2000) with a He-Cd laser (λ = 325 nm) as the excitation source. PL spectra were collected from three locations of the same samples and averaged to minimize the fluctuation in sample uniformity and measurements. TRPL data were collected from the UV peak around 377 nm at room temperature by time-correlated single photon counting (PicoQuantPicoHarp 300), excited by a 260 nm laser pulses (100 fs, 80 MHz) from the third harmonic of the Titanium sapphire laser (Chameleon, Coherent Inc.). XPS measurements were performed using VG ESCALAB 220i-XL instrument equipped with a monochromatic Al Ka (1486.7 eV) X-ray source.

Supporting Information

Supporting Information is available from the Wiley Online Library or from the author.

Acknowledgements

This work was mainly supported by the National University of Singapore and the Agency for Science, Technology and Research in Singapore. R.C. acknowledges the support from Natural Science Foundation of China (NSFC) under Grant No. 11404161. In addition, X.H. acknowledges Dr. Xiang Zhou for his critical comments on the manuscript.

Received: January 18, 2016
Revised: February 10, 2016
Published online: March 15, 2016

[1] K. Okamoto, I. Niki, A. Shvartser, Y. Narukawa, T. Mukai, A. Scherer, *Nat. Mater.* **2004**, *3*, 601.
[2] T. P. H. Sidiropoulos, R. Roder, S. Geburt, O. Hess, S. A. Maier, C. Ronning, R. F. Oulton, *Nat. Phys.* **2014**, *10*, 870.
[3] Q. Zhang, G. Li, X. Liu, F. Qian, Y. Li, T. C. Sum, C. M. Lieber, Q. Xiong, *Nat. Commun.* **2014**, *5*, 4953.
[4] J. Yoo, X. Ma, W. Tang, G.-C. Yi, *Nano Lett.* **2013**, *13*, 2134.
[5] S. Chu, G. Wang, W. Zhou, Y. Lin, L. Chernyak, J. Zhao, J. Kong, L. Li, J. Ren, J. Liu, *Nat. Nano* **2011**, *6*, 506.
[6] C. W. Cheng, E. J. Sie, B. Liu, C. H. A. Huan, T. C. Sum, H. D. Sun, H. J. Fan, *Appl. Phys. Lett.* **2010**, *96*, 071107.
[7] C. Chen, H. P. He, Y. F. Lu, K. W. Wu, Z. Z. Ye, *ACS Appl. Mater. Interfaces* **2013**, *5*, 6354.
[8] X. H. Huang, Z. Y. Zhan, K. P. Pramoda, C. Zhang, L. X. Zheng, S. J. Chua, *CrystEngComm* **2012**, *14*, 5163.
[9] R. Chen, Q. L. Ye, T. C. He, V. D. Ta, Y. J. Ying, Y. Y. Tay, T. Wu, H. D. Sun, *Nano Lett.* **2013**, *13*, 734.
[10] Z. L. Wang, *J. Phys.: Condens. Matter* **2004**, *16*, R829.
[11] M. M. Brewster, X. Zhou, M. Yen Lu, a. S. Gradecak, *Nanoscale* **2012**, *4*, 1455.
[12] A. B. Djurisic, Y. H. Leung, *Small* **2006**, *2*, 944.
[13] L. Li, S. S. Pan, X. C. Dou, Y. G. Zhu, X. H. Huang, Y. W. Yang, G. H. Li, L. D. Zhang, *J. Phys. Chem. C* **2007**, *111*, 7288.
[14] H. B. Zeng, G. T. Duan, Y. Li, S. K. Yang, X. X. Xu, W. P. Cai, *Adv. Funct. Mater.* **2010**, *20*, 561.
[15] X. H. Huang, C. B. Tay, Z. Y. Zhan, C. Zhang, L. X. Zheng, T. Venkatesan, S. J. Chua, *CrystEngComm* **2011**, *13*, 7032.
[16] G. P. Li, R. Chen, D. L. Guo, L. M. Wong, S. J. Wang, H. D. Sun, T. Wu, *Nanoscale* **2011**, *3*, 3170.
[17] A. Dev, J. P. Richters, J. Sartor, H. Kalt, J. Gutowski, T. Voss, *Appl. Phys. Lett.* **2011**, *98*, 131111.
[18] Q. J. Ren, S. Filippov, S. L. Chen, M. Devika, N. K. Reddy, C. W. Tu, W. M. Chen, I. A. Buyanova, *Nanotechnology* **2012**, *23*, 425201.
[19] A. Kuzma, M. Weis, S. Flickyngerova, J. Jakabovic, A. Satka, E. Dobrocka, J. Chlpik, J. Cirak, M. Donoval, P. Telek, F. Uherek, D. Donoval, *J. Appl. Phys.* **2012**, *112*, 103531.
[20] C. C. Li, K. L. Shuford, M. H. Chen, E. J. Lee, S. O. Cho, *ACS Nano* **2008**, *2*, 1760.
[21] J. Huang, K. H. P. Tung, L. Deng, N. Xiang, J. Dong, A. J. Danner, J. Teng, *Opt. Mater. Express* **2013**, *3*, 2003.
[22] R. Liu, X. W. Fu, J. Meng, Y. Q. Bie, D. P. Yu, Z. M. Liao, *Nanoscale* **2013**, *5*, 5294.
[23] S. Mukherjee, F. Libisch, N. Large, O. Neumann, L. V. Brown, J. Cheng, J. B. Lassiter, E. A. Carter, P. Nordlander, N. J. Halas, *Nano Lett.* **2013**, *13*, 240.
[24] C. Clavero, *Nat. Photon.* **2014**, *8*, 95.
[25] M. L. Brongersma, N. J. Halas, P. Nordlander, *Nat. Nano* **2015**, *10*, 25.
[26] X. H. Huang, C. Zhang, C. B. Tay, T. Venkatesan, S. J. Chua, *Appl. Phys. Lett.* **2013**, *102*, 111106.
[27] R. Sundararaman, P. Narang, A. S. Jermyn, W. A. Goddard Iii, H. A. Atwater, *Nat. Commun.* **2014**, *5*, 5788.
[28] E. Ringe, M. R. Langille, K. Sohn, J. Zhang, J. X. Huang, C. A. Mirkin, R. P. Van Duyne, L. D. Marks, *J. Phys. Chem. Lett.* **2012**, *3*, 1479.
[29] K. W. Liu, Y. D. Tang, C. X. Cong, T. C. Sum, A. C. H. Huan, Z. X. Shen, L. Wang, F. Y. Jiang, X. W. Sun, H. D. Sun, *Appl. Phys. Lett.* **2009**, *94*, 151102.
[30] R. Dingle, *Phys. Rev. Lett.* **1969**, *23*, 579.
[31] S. K. Lee, S. L. Chen, D. Hongxing, L. Sun, Z. Chen, W. M. Chen, I. A. Buyanova, *Appl. Phys. Lett.* **2010**, *96*, 083104.
[32] A. Teke, U. Ozgur, S. Dogan, X. Gu, H. Morkoc, B. Nemeth, J. Nause, H. O. Everitt, *Phys. Rev. B* **2004**, *70*, 195207.
[33] D. L. Shao, H. T. Sun, M. P. Yu, J. Lian, S. Sawyer, *Nano Lett.* **2012**, *12*, 5840.
[34] Y. Zhang, A. Dragan, C. D. Geddes, *J. Phys. Chem. C* **2009**, *113*, 12095.
[35] V. A. Fonoberov, K. A. Alim, A. A. Balandin, F. X. Xiu, J. L. Liu, *Phys. Rev. B* **2006**, *73*, 165317.
[36] D. C. Look, D. C. Reynolds, C. W. Litton, R. L. Jones, D. B. Eason, G. Cantwell, *Appl. Phys. Lett.* **2002**, *81*, 1830.
[37] T. Schmidt, K. Lischka, W. Zulehner, *Phys. Rev B* **1992**, *45*, 8989.
[38] G. Z. Xing, G. C. Xing, M. J. Li, E. J. Sie, D. D. Wang, A. Sulistio, Q. L. Ye, C. H. A. Huan, T. Wu, T. C. Sum, *Appl. Phys. Lett.* **2011**, *98*, 102105.
[39] S. Y. Jin, H. J. Son, O. K. Farha, G. P. Wiederrecht, J. T. Hupp, *J. Am. Chem. Soc.* **2013**, *135*, 955.
[40] A. Manjavacas, J. G. Liu, V. Kulkarni, P. Nordlander, *ACS Nano* **2014**, *8*, 7630.
[41] M. J. Feldstein, C. D. Keating, Y. H. Liau, M. J. Natan, N. F. Scherer, *J. Am. Chem. Soc.* **1997**, *119*, 6638.
[42] A. Y. Polyakov, N. B. Smirnov, E. A. Kozhukhova, V. I. Vdovin, K. Ip, Y. W. Heo, D. P. Norton, S. J. Pearton, *Appl. Phys. Lett.* **2003**, *83*, 1575.
[43] H. M. Chen, C. K. Chen, C.-J. Chen, L.-C. Cheng, P. C. Wu, B. H. Cheng, Y. Z. Ho, M. L. Tseng, Y.-Y. Hsu, T.-S. Chan, J.-F. Lee, R.-S. Liu, D. P. Tsai, *ACS Nano* **2012**, *6*, 7362.
[44] A. Hoggard, L. Y. Wang, L. L. Ma, Y. Fang, G. You, J. Olson, Z. Liu, W. S. Chang, P. M. Ajayan, S. Link, *ACS Nano* **2013**, *7*, 11209.
[45] A. Furube, L. Du, K. Hara, R. Katoh, M. Tachiya, *J. Am. Chem. Soc.* **2007**, *129*, 14852.
[46] K. Schouteden, Y.-J. Zeng, K. Lauwaet, C. P. Romero, B. Goris, S. Bals, G. Van Tendeloo, P. Lievens, C. Van Haesendonck, *Nanoscale* **2013**, *5*, 3757.
[47] X. Wang, X. G. Kong, Y. Yu, H. Zhang, *J. Phys. Chem. C* **2007**, *111*, 3836.
[48] C. Langhammer, Z. Yuan, I. Zoric, B. Kasemo, *Nano Lett.* **2006**, *6*, 833.
[49] W. M. Kwok, A. B. Djurišić, Y. H. Leung, W. K. Chan, D. L. Phillips, *Appl. Phys. Lett.* **2005**, *87*, 093108.
[50] A. B. Djurišić, W. M. Kwok, Y. H. Leung, D. L. Phillips, W. K. Chan, *J. Phys. Chem. B* **2005**, *109*, 19228.
[51] K. Okamoto, I. Niki, A. Scherer, Y. Narukawa, T. Mukai, Y. Kawakami, *Appl. Phys. Lett.* **2005**, *87*, 071102.
[52] M. M. Brewster, X. A. Zhou, S. K. Lim, S. Gradecak, *J. Phys. Chem. Lett.* **2011**, *2*, 586.
[53] L. Hu, L. P. Zhu, H. P. He, Y. M. Guo, G. Y. Pan, J. Jiang, Y. Z. Jin, L. W. Sun, Z. Z. Ye, *Nanoscale* **2013**, *5*, 9577.
[54] N. Zhang, W. Tang, P. Wang, X. T. Zhang, Z. Y. Zhao, *CrystEngComm* **2013**, *15*, 3301.
[55] S. T. Kochuveedu, J. H. Oh, Y. R. Do, D. H. Kim, *Chem. Eur. J.* **2012**, *18*, 7467.
[56] M. J. Kale, P. Christopher, *Science* **2015**, *349*, 587.